Paper ID: 268

Study of morphological and antimicrobial analysis of green synthesized Cu-doped Co-Zn oxide nanoparticles using *Mikania micrantha* (leaf) extract

Jahidul Alam Tanvir[1*], Md. Mosiul Haque[1], Shaadnan Bin Syed[1], Zahid Hasan[1]
[1]Rajshahi University of Engineering & Technology
**Corresponding author: E-mail: jahidulalamtanvir87@gmail.com; Phone:+880196-5660119*

Abstract

In the field of nanotechnology, particularly in the application of therapeutic, drug transporters, and drug delivery, eco-friendly nanoparticle production techniques have become increasingly popular. In this study, a green route was used for synthesizing Cu-doped Co-ZnO nanoparticles using Mikania micrantha (leaf) extract, characterized through XRD, SEM, and EDS analyses and antibacterial evaluation was done against gram-positive S. aureus and gram-negative E. coli bacteria using the Zone of Inhibition (ZOI) test. The XRD analysis confirmed that the nanoparticles exhibited a wurtzite hexagonal structure, and the cell volume increased with Cu doping (From 35.58Å^3 to 35.84Å^3). The SEM image confirmed that the synthesized particles were in the nanometer range (43.65nm and 28.53nm) and showed the agglomerated, almost spherical-like morphology of Cu-doped Co-Zn oxide nanoparticles. EDS diagrams revealed the chemical compositions of both doped and undoped particles, while the ZOI test demonstrated and compared the antibacterial efficacy of the samples.

Keywords: Zn nanoparticles, Green-synthesis, Mikania micrantha, Antimicrobial, Morphological analysis,

1. Introduction

In recent years, nanoscience and nanotechnology have seen remarkable advancements, particularly in medical applications. There is growing optimism that nanotechnology will lead to significant progress in disease diagnosis, treatment, drug delivery, and the development of biocompatible materials [1]. Cell-specific targeting is possible by linking drugs to custom-designed carriers. Advances in nanotechnology reveal that nanoparticles, typically under 100 nm in size, hold significant potential as drug-delivery systems [2]. Metallic nanoparticles are favored by researchers for their versatility across applications such as catalysis, sensors, electronics, and biomedicine [3]. Besides, their antibacterial characteristics have made them ideal candidates for antimicrobial, antiviral and drug-delivery applications [4, 5]. ZnO, known for its semiconductor properties, generates electron-hole pairs under UV light exposure, leading to the development of hydroxyl radicals and reactive oxygen species (ROS) [6]. These ROS are effective in killing bacteria by disrupting their protein chains. Cobalt is considered an effective dopant for the ZnO framework due to its abundant electron availability and high dissolvability [7, 8]. Co^{2+} ions readily substitute Zn^{2+} ions in the ZnO lattice, as the radius of the ion of Co is similar to that of Zn [9].

This article investigates Co-ZnO as the base material, with Cu doping applied to study its morphological and antimicrobial changes. Opting for a green synthesis route, Mikania micrantha leaf extract was used to synthesize Cu-doped Co-ZnO nanoparticles. As *Mikania micrantha* is abundant in Bangladesh and known to contain flavonoids, terpenoids, and phenolic compounds like quinones, its leaf extract can facilitate the reduction of metal ions and form nanoparticles [10]. The existence of quinones and plastohydroquinone molecules in the plant extract suggests that extracellular synthesis of metal nanoparticles can be accomplished using plant biomolecules and heterocyclic compounds [11]. Among the various processes for synthesizing nanoparticles, co-precipitation was selected for its simplicity, reduced time and energy requirements, and ability to produce homogeneous nanoparticles [12].

So, in this article, Cu was doped with Co-ZnO nanoparticles ($Cu_xCo_{1-x}ZnO$; x=0.15) using *M. micrantha* leaf extract as a capping agent and the co-precipitation method. The synthesized nanoparticles will be subjected to XRD, SEM, EDS, and ZOI tests to analyze their structural, physical, and antimicrobial characteristics.

2. Materials and methods

Materials

In this study, all constituents used were of analytical grade and were applied without further purification. The Zinc (II) nitrate hexahydrate ($Zn(NO_3)_2{\cdot}6H_2O$) (Purity: 96% Origin: India), Copper (II) nitrate trihydrate ($Cu(NO_3)_2.3H_2O$) (Purity: 98%, Origin: India), Cobalt (II) nitrate hexahydrate ($Co(NO_3)_2{\cdot}6H_2O$) (Purity: 97%, Origin: India), Sodium hydroxide (NaOH), and distilled water (DW) were obtained commercially. Fresh *M. micrantha* leaves were collected from the local area.

Methodology

To prepare the leaf extract, the leaves were rinsed 3-4 times with distilled water, finely chopped, and blended. The mixture was then filtered through Whatman filter paper, and the extract was stored at 5°C for subsequent use.

To prepare the nanoparticles, stoichiometric amounts of zinc nitrate and cobalt nitrate for Co-ZnO (CZ), and nitrate salts of Zn, Co, and Cu for $Cu_xCo_{1-x}ZnO$ (x=0.15) (CCZ) were dissolved in 100 ml of DW to form a consistent solution. After stirring for 30 minutes, the leaf extract was added in a 1:3 ratio at room temperature, and the mixture was magnetically stirred. It was then heated at 60-70°C for 3 hours while NaOH was gradually added to maintain the pH at 10-11. The resulting residue was separated by centrifugation at 3500 rpm, washed with distilled water and ethanol three times, and air-dried at 80°C for 24 hours. Lastly, the dried nanoparticles were calcined at 420°C for 1.5 hours, yielding Co-ZnO and Cu-doped Co-ZnO nanoparticles. The particles were analyzed for their structural, morphological, and antibacterial properties using XRD, SEM, EDS, and ZOI tests.

3. Characterization of nanoparticles

XRD analysis

The phase composition and structural properties of $Cu_xCo_{1-x}ZnO$ (x = 0.15) samples were analyzed at 25°C using a Bruker X-ray diffractometer with Cu Kα radiation (λ = 1.5406 Å), operating at 30 mA and 40 kV. The Scherrer equation offers an initial estimation of the crystallite size, as shown in the following equation:

$$D = \frac{k\lambda}{\beta cos\theta} \tag{1}$$

Here, 'D' denotes the average crystallite size, measured in units corresponding to the wavelength (λ). 'k' is the crystallite shape factor (0.89), 'β' represents the full width at half maximum (FWHM) of the peak in radians (2π) after correcting for instrumental effects, and 'θ' refers to the peak position. Additionally, the lattice parameters (a and c) were determined using the following relation:

$$\frac{1}{d^2} = \frac{h^2+k^2}{a^2} + \frac{l^2}{c^2} \tag{2}$$

SEM and EDS analysis

Scanning electron micrographs were obtained using a ZEISS (Model 14, Germany) electron microscope operating at a 5 kV accelerating voltage. The average grain size was resolved from SEM images using ImageJ software, with measurements taken from approximately 80 individual grains. Elemental analysis of the nanoparticles was performed using an EDS instrument.

Zone of inhibition (ZOI) analysis

Using the agar well diffusion method, the antimicrobial efficacy of CZ and Cu-doped CZ nanoparticles was evaluated against gram-positive bacteria (*Staphylococcus aureus*) and gram-negative bacteria (*Escherichia coli*). A sterile agar medium was prepared in a conical flask at room temperature and subsequently inoculated with clinical samples of *S. aureus* and *E. coli* bacteria. This mixture was incubated at 40°C for 24 hours, ensuring even distribution of the bacterial cultures through stirring. After thorough mixing, the medium was poured into a sterile petri dish and allowed to solidify. Samples were then added to wells at concentrations of 25, 50, and 100 µg/mL. Ciprofloxacin (5 mg/mL) and methanol served as positive and negative controls. The antibacterial activity was assessed 24 hours post-incubation by measuring the inhibition zone diameter in millimeters.

4. Result analysis

XRD graph

The XRD spectra (Figure 1a) illustrate the diffraction patterns of CZ and CCZ nanoparticles synthesized via the co-precipitation technique, followed by calcination at 420°C. The XRD measurements were performed at room temperature, covering a 2θ-degree range from 25° to 75°. The observed peaks at 2θ = 31.78°, 34.44°, 36.27°, 56.65°, 63.42°, and 68.03°, corresponding to the Miller indices (100), (002), (101), (110), (103), and (201), indicate the presence of a wurtzite hexagonal structure (space group P63mc) in both CZ (JCPDS card no. 96-153-3021) and CCZ nanoparticles.

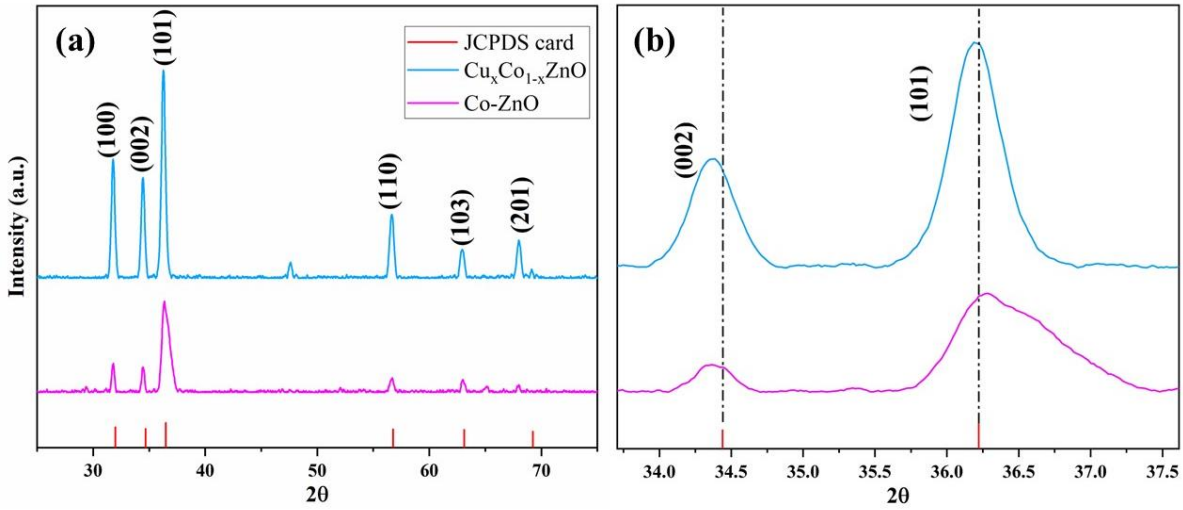


Figure 1. XRD analysis of CZ and CCZ nanoparticles: a) peak positions and miller indices, and b) peak shift of two major peaks.

Figure 1a illustrates that the doping of Cu into the Co-ZnO matrix leads to an uprise in peak intensity, representing an improvement in both crystallite size and crystallinity of the doped sample (Table 1). In Figure 1b, a slight shift in the positions of the two prominent peaks, (002) and (101), is observed for the doped sample towards lower 2θ values compared to the undoped sample. This minor shift corresponds to a slight increase in the lattice parameters and unit cell volume, as detailed in Table 1.

Table 1. Different parameters achieved from XRD data.

Materials	D (nm)	Lattice parameter (Å)		c/a ratio	Unit cell volume (Å^3)	Crystallinity
		a	c			
Co-ZnO	19.87	2.81	5.203	1.85	35.58	74.65%
$Cu_{0.15}Co_{0.85}ZnO$	22.78	2.82	5.205	1.85	35.84	83.86%

Morphological analysis

The surface morphology of CZ and CCZ nanoparticles was observed through SEM studies. Figure 2 shows the SEM images of the un-doped CZ and 0.15 wt% CCZ samples, respectively. Small, almost spherical aggregates of smaller individual nanoparticles are shown in these images. From Figure 2a, it is clearly observed that un-doped Co-ZnO nanoparticles have grain sizes average of 43.65nm with inter-granular spacing. The average particle size of these nanoparticles was found to be 28.53 nm for 0.15% Cu-doped Co-ZnO. Figure 2b also revealed that agglomerated spherical shapes were observed in the SEM image of CCZ. The observations indicate that the Cu concentration influences the parent Co-ZnO, with the grain size remaining within the nanoscale range. Still, the slight addition of Cu concentration decreases the particle size.

The EDS spectrum shown in Figure 3 confirms the presence of Zinc, Cobalt, Copper, and Oxygen in the sample. The compositional analysis of the samples was determined using EDS spectroscopy, and Zn, O, and Co were the primary elements with evidence of the doping element (Copper) in the spectrum. This validated the high purity of the integrated CCZ. According to theoretical predictions, Zn and Co should have an increased stoichiometric weight percentage, while Co should be present in a smaller proportion. The upsurge in Zn, O, and Co levels seen in Figure 3a & b following Cu^{2+}-doping can be attributed to alterations in the crystalline arrangement and

oxidation states caused by the incorporation of Cu into the Co-Zn matrix. Therefore, the compositional analysis reveals a rise in Cu, demonstrating these structural modifications. The consequences of the EDS analysis align with these predictions for the nanoparticles that are produced.

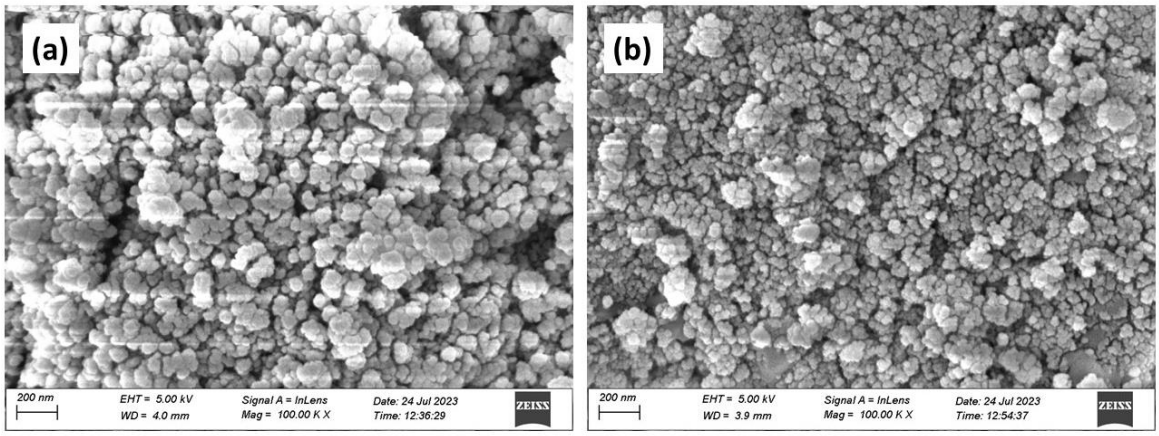
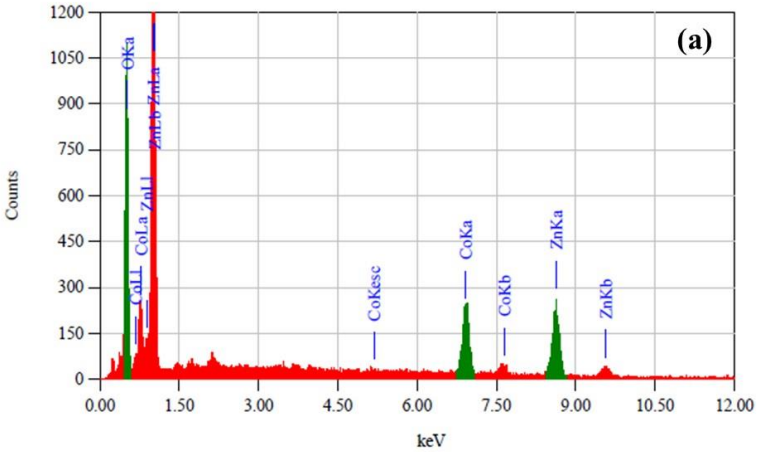
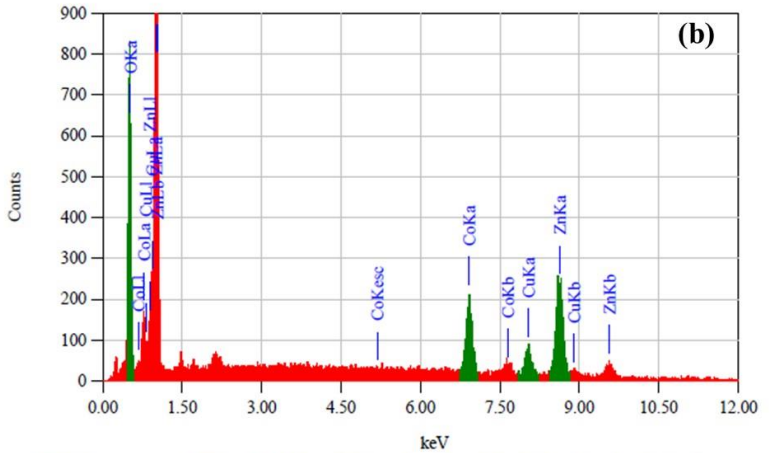


Figure 2. SEM image of a) CZ and b) CCZ nanoparticles at 100kx magnification.



Element	(keV)	Mass%	Sigma	Atom%	Compound	Mass%	Cation	K
O K	0.525	24.75	0.33	56.64				25.6709
Co K	6.924	19.83	0.46	12.32				21.1314
Zn K	8.630	55.42	1.25	31.04				53.1977
Total		100.00		100.00				



Element	(keV)	Mass%	Sigma	Atom%	Compound	Mass%	Cation	K
O K	0.525	18.55	0.28	47.63				18.6513
Co K	6.924	14.33	0.38	9.99				15.8677
Cu K	8.040	10.78	0.47	6.97				10.5060
Zn K	8.630	56.34	1.22	35.41				54.9749
Total		100.00		100.00				

Figure 3. EDS spectra of a) CZ and b) CCZ nanoparticles.

Antimicrobial analysis

The antimicrobial efficacy of CZ and CCZ was examined against *S. aureus* and *E. coli* at concentrations of 25, 50, and 100 μg/mL. Figure 4 demonstrates that the nanoparticles exhibit exceptional antibacterial characteristics compared to the standard antibiotics Ciprofloxacin and methanol. CZ nanoparticles exhibit very little and irregular antibacterial activity. Doping of Cu ion to the Co-ZnO matrix greatly increased the antibacterial activity, especially at higher concentrations (Table 2). So, in conclusion, Co-ZnO nanoparticles showed a very poor and irregular inhibition zone, whereas Cu-doped Co-ZnO nanoparticles have shown enhanced antibacterial capabilities.

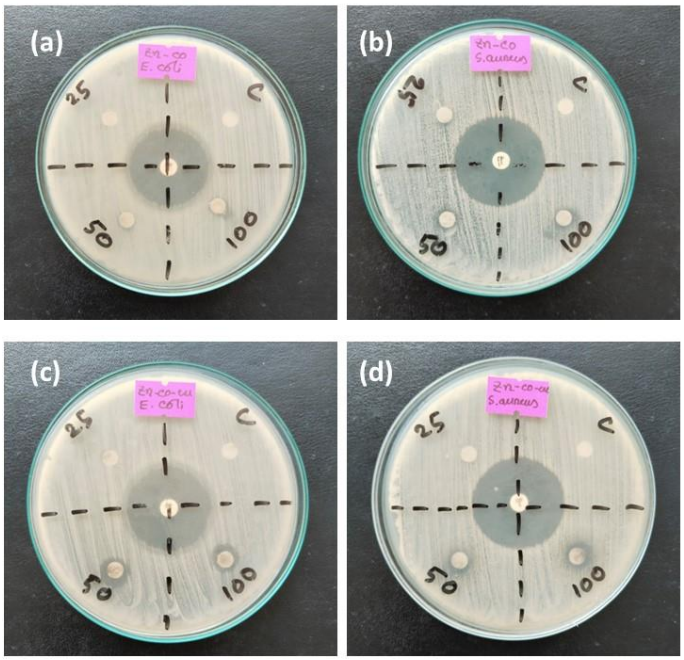


Figure 4. Antibacterial activity plate photos of CZ nanoparticles against a) *E. coli*, b) *S. aureus*, and CCZ nanoparticles against c) *E. coli*, d) *S. aureus.*

Table 2. Antibacterial zone measurements of nanoparticle sample

Sample	Concentration (μg/mL)	ZOI (mm)	
		E. coli	*S. aureus*
Co-ZnO	25	0	0
	50	1.5±0.5	2±0.3
	100	1±0.8	3±0.8
	Ciprofloxacin	27	31
	Methanol	---	---
$Cu_{0.15}Co_{0.85}ZnO$	25	0	0
	50	8.5±0.2	7.5±0.5
	100	10±0.3	9±0.2
	Ciprofloxacin	27	31
	Methanol	---	---

5. Conclusion

In this experiment, Cu was successfully doped with Co-ZnO nanoparticles using *Mikania micrantha* leaf extract and the co-precipitation method. XRD analysis confirmed the wurtzite hexagonal structure of the synthesized nanoparticles, while SEM imaging, at various magnifications, verified their nanoscale size and revealed an agglomerated, nearly spherical morphology in the Cu-doped Co-ZnO nanoparticles. EDS analysis further elucidated the chemical composition of both doped and undoped samples. Additionally, the ZOI test demonstrated the antibacterial effectiveness of the nanoparticles, highlighting a comparative enhancement in antimicrobial properties for the Cu-doped samples. Further tests, such as photocatalytic analysis, will provide conclusive insights into their potential future applications.

6. Acknowledgement

The authors acknowledge Md. Manwar Hossain, Technical officer, Department of Glass & Ceramic Engineering, Rajshahi University of Engineering & Technology (RUET).

7. References

[1] de Jong, “Drug delivery and nanoparticles: Applications and hazards,” *Int J Nanomedicine*, p. 133, Jun. 2008, doi: 10.2147/IJN.S596.

[2] A. Z. Wilczewska, K. Niemirowicz, K. H. Markiewicz, and H. Car, “Nanoparticles as drug delivery systems,” *Pharmacological Reports*, vol. 64, no. 5, pp. 1020–1037, Sep. 2012, doi: 10.1016/S1734-1140(12)70901-5.

[3] A. Bankar, B. Joshi, A. Ravi Kumar, and S. Zinjarde, “Banana peel extract mediated synthesis of gold nanoparticles,” *Colloids Surf B Biointerfaces*, vol. 80, no. 1, pp. 45–50, Oct. 2010, doi: 10.1016/j.colsurfb.2010.05.029.

[4] M. H. Rashid, S. I. Sujoy, M. S. Rahman, and M. J. Haque, “Aloe vera assisted green synthesis of Ag and Cu co-doped ZnO nanoparticles and a comprehensive analysis of their structural, morphological, optical, electrical and antibacterial properties,” *Heliyon*, vol. 10, no. 3, p. e25438, Feb. 2024, doi: 10.1016/j.heliyon.2024.e25438.

[5] M. A. Hassaan, A. I. Meky, H. A. Fetouh, A. M. Ismail, and A. El Nemr, “Central composite design and mechanism of antibiotic ciprofloxacin photodegradation under visible light by green hydrothermal synthesized cobalt-doped zinc oxide nanoparticles,” *Sci Rep*, vol. 14, no. 1, p. 9144, Apr. 2024, doi: 10.1038/s41598-024-58961-4.

[6] R. Ebrahimi *et al.*, “Effects of doping zinc oxide nanoparticles with transition metals (Ag, Cu, Mn) on photocatalytic degradation of Direct Blue 15 dye under UV and visible light irradiation,” *J Environ Health Sci Eng*, vol. 17, no. 1, pp. 479–492, Jun. 2019, doi: 10.1007/s40201-019-00366-x.

[7] B. Liu and H. C. Zeng, “Hydrothermal Synthesis of ZnO Nanorods in the Diameter Regime of 50 nm,” *J Am Chem Soc*, vol. 125, no. 15, pp. 4430–4431, Apr. 2003, doi: 10.1021/ja0299452.

[8] K. Tanji *et al.*, “Design and simulation of a photocatalysis reactor for rhodamine B degradation using cobalt-doped ZnO film,” *Reaction Kinetics, Mechanisms and Catalysis*, vol. 134, no. 2, pp. 1017–1038, Dec. 2021, doi: 10.1007/s11144-021-02116-3.

[9] M. Rezaei and A. Nezamzadeh-Ejhieha, “The ZnO-NiO nano-composite: A brief characterization, kinetic and thermodynamic study and study the Arrhenius model on the sulfasalazine photodegradation,” *Int J Hydrogen Energy*, vol. 45, no. 46, pp. 24749–24764, Sep. 2020, doi: 10.1016/j.ijhydene.2020.06.258.

[10] A. Al Mahmood, S. Bin Syed, Z. Hasan, M. B. Islam, R. Hossain, and S. Rahman, “Structural, morphological, optical, and antimicrobial study of Mikania micrantha (leaf) extract treated zinc doped cobalt ferrite nanoparticles and antibacterial clothing applications,” *Results in Surfaces and Interfaces*, p. 100303, Sep. 2024, doi: 10.1016/j.rsurfi.2024.100303.

[11] J. Kesharwani, K. Y. Yoon, J. Hwang, and M. Rai, “Phytofabrication of Silver Nanoparticles by Leaf Extract of <I>Datura metel</I>: Hypothetical Mechanism Involved in Synthesis,” *Journal of Bionanoscience*, vol. 3, no. 1, pp. 39–44, Jun. 2009, doi: 10.1166/jbns.2009.1008.

[12] I. H. Gul, A. Z. Abbasi, F. Amin, M. Anis-ur-Rehman, and A. Maqsood, “Structural, magnetic and electrical properties of Co1−xZnxFe2O4 synthesized by co-precipitation method,” *J Magn Magn Mater*, vol. 311, no. 2, pp. 494–499, Apr. 2007, doi: 10.1016/j.jmmm.2006.08.005.